Heating and Current Drive by Electron Cyclotron Waves in JT-60U

T. Suzuki 1), S. Ide 1), C. C. Petty 2), Y. Ikeda 1), K. Kajiwara 1), A. Isayama 1),
K. Hamamatsu 1), O. Naito 1), M. Seki 1), S. Moriyama 1) and the JT-60 Team 1)

1) Japan Atomic Energy Research Institute, Naka-machi, Naka-gun, Ibaraki 311-0193, Japan
2) General Atomics, San Diego, California, US

e-mail contact of main author: suzukit@fusion.naka.jaeri.go.jp

Abstract. Results of studies on heating and current drive by the electron cyclotron (EC) waves in JT-60U are presented. Electron temperature up to 26keV was achieved by injecting EC waves in the center of a reversed shear plasma produced by the lower hybrid (LH) waves. The electron temperature T_e exceeds 24keV in a wide range of minor radius ($\rho<0.3$, where ρ is the normalized minor radius). ECCD (Current Drive) efficiency η_{CD} was examined at high T_e up to 21keV without using LH waves. The CD efficiency increases with T_e, but there is discrepancy from linear dependence on T_e in a high T_e regime of 10-20keV. Dependence of normalized CD efficiency $\zeta=e^3\eta_{CD}/\varepsilon_0^2 kT_e$ on deposition location was also studied to optimize the CD efficiency, since trapped particle effect, which depends strongly on deposition location, is expected to reduce ζ. The effect was detected from significant decrease in ζ in the lower magnetic field deposition, which is consistent with linearlized Fokker-Planck calculation.

1. Introduction

Electron cyclotron (EC) waves are considered as a strong tool to control electron heating and current profile in plasmas. Since EC waves are absorbed by electron cyclotron resonance, it is considered that absorption location of waves can be easily determined by calculation, so that heating and current drive only close to the resonance is possible. Actually, EC driven current profiles have been measured in DIII-D [1] and in JT-60U [2,3], and it was shown that the measured EC driven current profiles are spatially localized and that they agree with calculations at least in moderate conditions. Owing to such advantages, EC systems are planned to be installed in ITER (International Thermonuclear Experimental Reactor). Main purposes of EC system in ITER were described as follows [4,5]. 1) Steady state current drive capability. 2) Assistance of plasma control, especially to stabilize neo-classical tearing mode (NTM). 3) Wall conditioning. 4) Assistance of the poloidal field system in breakdown and current initiation phase. 5) Heating source to access H-mode.

In this paper, we treat the first and the second ones. The former concerns to on-axis current drive by EC waves (ECCD) in high electron temperature plasmas. Existing data are limited up to T_e ~7keV in T-10 [6] and in JT-60U [2], while ECCD is expected in volume averaged T_e under 12keV in ITER. Electron temperature at CD location in ITER should be much higher than 12keV in on-axis ECCD case. In such high T_e regime, apart from linear dependence of current drive efficiency on T_e is expected [5,7]. The second one concerns off-axis ECCD, since NTMs usually occur around m/n=2/1 or 3/2 (poloidal / toroidal mode numbers) surfaces. NTMs on such a major rational surface usually accompany larger islands and affect the plasma confinement. The major rational surface exists in off-axis, where it is considered that trapped particles affect ECCD efficiency, if low-q operation is employed aiming economically preferable high β operation. The effect should be studied for applicable use of ECCD for NTM suppression [8].

Section 2 describes recent progress of EC system in JT-60U and production of high T_e plasma using EC waves. On-axis ECCD in such high T_e plasma is analyzed in Section 3. CD efficiency is investigated as a function of electron temperature close to the ITER operation regime. Section 4 describes off-axis ECCD in relation to the trapped particle effect. The effect

is experimentally investigated by changing the deposition location. Dependence of CD efficiencies on electron density and electron temperature is also described. The dependence can help to find optimized plasma parameters for ECCD. EC driven current profile in a large minor radius is also studied, where trapped particle fraction is close to that in ITER. Summary is in the section 5.

2. Progress of EC System in JT-60U and Production of High Electron Temperature plasma

JT-60U has four units of EC systems, each of which has one gyrotron with frequency of 110GHz [9,10]. One unit of them was installed in 2000. EC waves are injected into plasma from lower field side of torus (upper outboard) usually as an O-mode. EC waves are absorbed in fundamental resonance for about 4T of toroidal field. These conditions are same as ITER, except the wave frequency and the toroidal field. Toroidal injection angle of an antenna, which three units of gyrotrons use, is fixed with an angle so that the refractive index parallel to magnetic field $N_{//}$ is about 0.5 at the plasma center. The angle is about 60° to the direction of toroidal field at the plasma center. Another antenna for the newly installed unit has a capability to control toroidal injection angle for co-/ctr-ECCD or for just heating. Both antennas can change injection angle in poloidal cross-section to control deposition location. EC system in JT-60U has extended the injection power P_{in} into the plasma up to 3MW for 2.7s. The pulse duration reached 5s at 1.5MW. Energy injected into the plasma reached 10MJ (2.8MW for 3.6s); see Fig. 1. Output power per a gyrotron was about 1MW, and transmission efficiency was 70-80%. The output power per a gyrotron and transmission efficiency were close to that required for EC system in ITER, although ITER is designed to use more gyrotrons. Not only the additional fourth unit of EC system but also the increases of the output power and of the transmission efficiency contribute the increase of P_{in}.

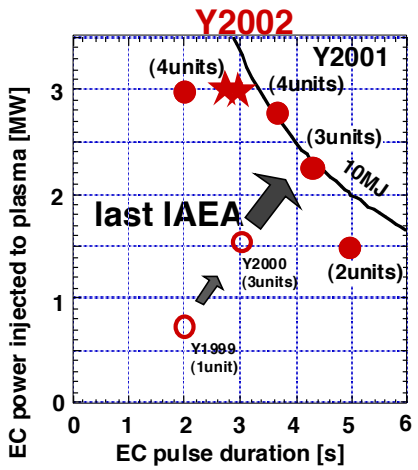

FIG. 1. Progress in the EC power injected into plasma and in its pulse duration in JT-60U. Closed circles and stars represent achieved results in 2001 and in 2002, respectively.

The progress in the input power made it possible to produce plasmas with high T_e up to 26keV measured by the ECE diagnostics [11]. Error in ECE measurement was typically ±2keV in this discharge. Temporal evolution of the electron temperature at the plasma center $T_e(0)$ is shown in Fig. 2 along with the heating power by EC (dashed) and LH (dotted) waves.

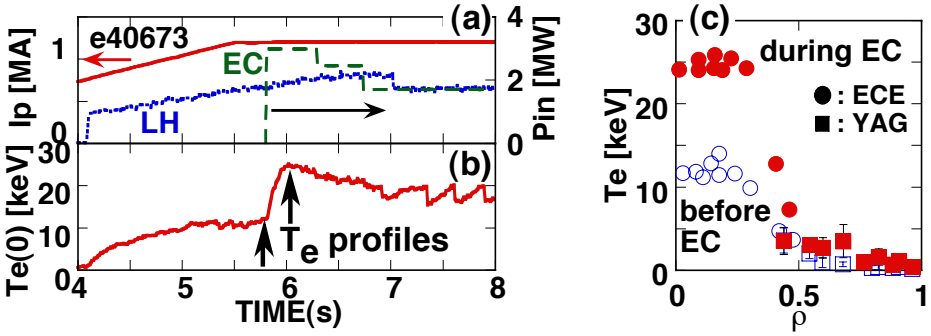

FIG. 2. Temporal evolutions of plasma current (I_p), injected power (P_{in}) (a) and the electron temperature at the plasma center (b). (c) T_e profile against the normalized minor radius. Open and closed symbols denote T_e before and during the EC, respectively. Circles and squares represent T_e measured by ECE and Thomson scattering by YAG LASER, respectively.

The profiles of the electron temperature before and during the EC heating are also shown in Fig. 2. Preheating by the LH waves [12] up to 1.9MW raised $T_e(0)$ to 12keV. LHCD was applied during the plasma current (I_p) ramp-up in order to produce a negative shear region in the center of the plasma [13,14]. The negative shear within $\rho<0.4$ is confirmed by the motional Stark effect (MSE) diagnostics [11] even at t=8.2s. When the EC waves of 2.9MW were put in the center of the plasma, electron temperature in the negative shear region exceeded 24keV in a wide range of minor radius ($\rho<0.3$), and was 26keV at the maximum.

3. On-axis ECCD in a Wide Range of Electron Temperature

Simultaneous current drive by EC waves and by LH waves can produce error in the determination of EC driven current due to the error in LH driven current [15] and synergetic effect with LH and EC waves. Therefore, we prefer discharges without LH waves for on-axis EC driven current measurement. Waveforms of a discharge are shown in Fig. 3(a). EC waves are put at the flat top phase of the plasma current of 0.6MA. Neutral beams (NBs) of about 1.7MW are for MSE diagnostics. Two units of NBs are put in balanced to cancel beam driven current. Central electron temperature measured by ECE increases up to 23keV, by injecting 2.9MW of EC waves. Line averaged electron density is nearly constant during the EC injection. Slight increase of the n_e after the EC injection is mainly due to the increased fueling by diagnostic NB for MSE as shown in Fig. 3(a). Loop voltage dropped to about 0.1V. We had stable plasma with such high T_e for about 0.8s until crash in T_e occurred at t=5.96s. In this series of experiment, duration without instability shortens when strong on-axis ECCD is applied. Therefore in this discharge, one unit of EC (0.6MW) is used for just heating, and three units of ECs (2.3MW) are used (and fixed) for co-ECCD. Measurement of EC driven current is made from t=5.5s to 5.9s, as hatched in Fig. 3(a). Electron temperature profile during the analysis is shown in Fig. 3(b). Although the central electron temperature is measured by ECE, we confirmed that Thomson scattered spectra of ruby LASER extremely broadened so that the electron temperature near the center is probably no less than 20keV.

Non-inductive current was evaluated by the loop voltage profile analysis [2,16] using the MSE in a high electron temperature plasma of $T_e(0)$=23keV with EC heating. The EC driven current profile is shown in Fig. 4(a), in comparison with a result of linearized Fokker-Planck calculation. The measured EC driven current profile is spatially localized even in the high T_e

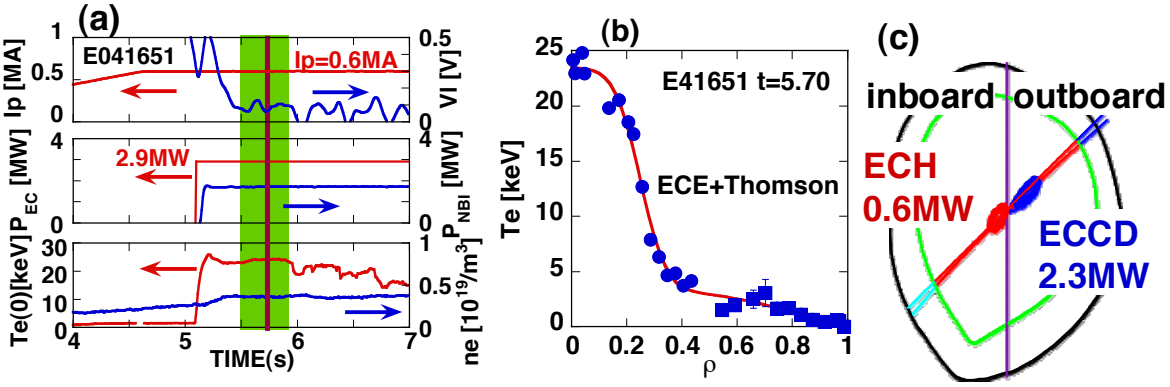

FIG. 3. (a) Waveforms of a discharge; plasma current (I_p), loop voltage (Vl), injected EC power (P_{EC}), NB heating power (P_{NBI}), electron temperature at plasma center ($T_e(0)$), line averaged electron density (n_e). EC driven current is evaluated during the hatched region (t=5.5-5.9s), where $T_e(0)$ is nearly constant. (b) Electron temperature profile during ECCD analysis at the t=5.7s. Electron temperature is measured by ECE (circles) and Thomson scattering (squares with errors) diagnostics. (c) Deposition locations of EC waves for current drive (LFS) and heating (HFS). Magnetic axis is between the two locations.

regime. The measured EC driven current I_{EC} was 0.74±0.06MA, where T_e at the CD location was 21keV. The CD location means a magnetic surface where enclosed EC driven current is a half of total EC driven current. Linearized Fokker-Planck code predicts I_{EC}=1.1MA. The calculation includes a trapped particle effect by toroidicity, but does not include an electric field effect by Ohmic field. The measurement was made in a transient phase (0.4-0.8s after the EC injection) during the inductive current diffusion. The resistive diffusion time for the width of the experimental EC driven current profile (standard deviation of Gaussian fit: 0.16m) is about 22s for T_e =21keV. Therefore, most of the EC driven current is canceled by the inductive electric field. When the EC driven current modifies the total current profile due to the diffusion of the inductive field, minimum of the safety factor approaches 2.5 (0.86s after the EC injection). Since some instability prevents evolution of the total current profile, apparent EC driven current (0.74MA) does not exceed plasma current (0.6MA); loop voltage of the plasma does not get negative as seen in Fig. 3(a). The instability is seen in the sudden decrease in T_e in Fig. 3(a) at t=5.96s.

Figure 5 shows the measured current drive efficiency $\eta_{CD} = I_{EC} R_p n_e / P_{abs}$ as a function of the electron temperature at CD location. In the above definition, R_p and P_{abs} are the major radius of plasma and absorbed power of EC waves used for current drive, respectively. The absorption power is defined as input power multiplied by absorption fraction of EC waves calculated by linearized Fokker-Planck calculation. Absorption fractions in Fig. 5 were more than 95%. All of the CD locations of data in Fig. 5 are $\rho \leq 0.17$. Calculated CD efficiency for the experimental condition is also plotted in the Fig. 5. Measured and calculated η_{CD} are found to increase with local T_e at CD location. The range in T_e covers considerable part of the ITER operation regime (12keV in volume averaged T_e). The highest CD efficiency was 0.42×10^{19} A/W/m^2. The experimental CD efficiency was smaller than that of calculation. There are candidates to produce the difference. One of them is the negative electric field that is produced by induction of EC driven current. Negative electric field in plasma is expected to reduce EC driven current and the efficiency [17]. Since the linearized Fokker Planck calculation do not include the effect, the calculation can be smaller in the experimental condition with negative electric field. In other words, ECCD in a fully steady state, where no electric field remains, will show higher experimental CD efficiency. Such an ECCD experiment will be a demonstration of ECCD in ITER. Since the evolution of the plasma current is limited by an instability as described before, it is important to avoid the instability

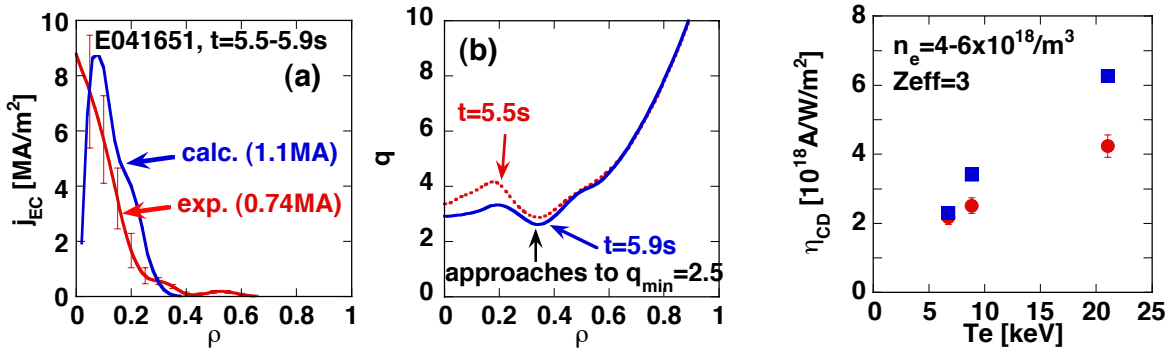

FIG. 4. (a) EC driven current profile of experimental measurement (exp.) and that of linearized Fokker-Planck calculation (calc.). Spatially integrated EC driven currents are also shown for both cases. (b) Safety factor profiles at the start (t=5.5s) and at the end (t=5.9s) of the loop voltage profile analysis. Since EC driven current in (a) increases the total current density in ρ<0.4, safety factor decreases around the magnetic axis. When q_{min} reaches to 2.5, some instability occurs.

FIG. 5. Measured ECCD efficiency (circle) in JT-60U increases with the electron temperature at CD location. Linearized Fokker-Planck calculations (square) also show the same tendency, while the measurements are smaller than the calculations.

to reduce the EC driven current. Combination of smaller ECCD and larger ECH will provide such a condition. Others are as follows. If distribution function of electron is strongly distorted by the perpendicular heating by EC waves, parallel temperature could be lower than the perpendicular one. Slower parallel velocity shifts the deposition location of EC waves, and hence CD location, more close to the magnetic axis, since ECCD location is LFS of plasma (Fig. 3(c)). Another candidate is an enhanced radial transport of wave coupled electrons [18]. The last one may not the case, since the characteristic scale width of the experimental EC driven current profile does not show broadening. In comparison between the experiment and the calculation, we should also consider non-linearity effect that is off course not included in the linear calculation. To achieve a high Te by ECH, electron density was small and absorption power density was large in the on-axis ECCD. A parameter p_{abs}/n_{e19}^2 exceeds a criterion of 0.5 under the experimental condition, which requires non-linear treatment of Fokker-Planck equation [19]. Notation p_{abs} and n_{e19}^2 are absorbed power density in MW/m^3 and electron density in 10^{19}m^{-3}, respectively. Comparison between the experiment and calculation should be investigated in future, considering the electric field effect and the non-linearity effect.

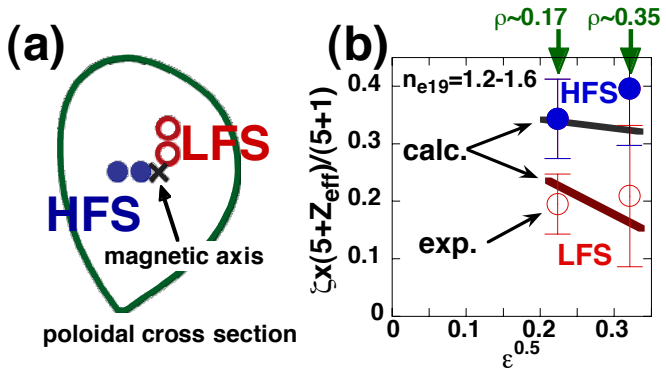

FIG. 6. (a) Schematic view of the CD location in the experiment. (b) Normalized current drive efficiency ζ against a measure of the trapped particle fraction $\varepsilon^{0.5}$ in LFS. The CD location in normalized minor radius ρ was about 0.17 and 0.35 respectively. Open and closed circles indicate deposition locations for LFS and for HFS, respectively in (a) and (b). Upper and lower lines in (b) show tendency of linearized Fokker-Planck calculation for the HFS and for the LFS, respectively.

4. Off-axis ECCD for Trapped Particle Effect Study

Properties of the EC driven current are studied in detail for a higher CD efficiency. Emphases are mainly put on the trapped particle effect, which is expected to reduce the normalized EC driven current efficiency $\zeta=e^3\eta_{CD}/\varepsilon_0^2 kT_e$. Principal dependencies of CD efficiency on plasma parameters are removed in ζ. Since the reduction of ζ affects the required EC power for the current profile control, the effect should be investigated. It is expected that the normalized CD efficiency is different between higher field side (HFS) deposition (smaller trapped particle effect) and lower field side (LFS) deposition (larger effect). Since the fraction of the trapped particle is considered to be a function of inverse aspect ratio ε, dependence of ζ on minor radius is also expected. Square root of ε can be a measure of the trapped particle fraction in LFS. Two curves in Fig. 6 show the expected ζ by the linearized Fokker-Planck calculations including the trapped particle effect. We plotted converted ζ equivalent to Z_{eff} of unity, assuming a conventional weak Z_{eff} dependence like $\zeta \propto 1/(5+Z_{eff})$. The measured effective charge in this experiment was between 1.5 and 1.9 so that the correction was small. The lower curve represents the LFS deposition, showing reduction in ζ with minor radius. The upper curve is for the HFS deposition, where no significant decrease in ζ. Circles (closed/open) denote measured ζ in HFS/LFS deposition respectively. They seem to agree with the calculated values. Significant decrease (by a half) in ζ is seen in the case of LFS deposition compared to that of HFS deposition at ρ=0.35. The reduction in ζ may show the trapped particle effect. Dependence of ζ on minor radius (or ε) was not clear, since variation of ε was not enough compared to the error in ζ.

We investigated the property of ECCD depending on plasma parameters, such as n_e and T_e. Since these parameters could affect the absorption of EC waves, we can expect some effect that could not be normalized by the general formulation of CD efficiency ζ. That is to say, parameter dependencies specific to physics of ECCD. To ensure that the trapped particle effect are same, we had several ECCD discharges with same toroidal field and injection angle of EC waves, but with different T_e and n_e. The input power of EC waves was increased to keep T_e constant at higher n_e (Fig. 7(a)), or electron temperature was changed by input power of EC waves under same n_e (Fig. 7(b)). We can see experimental ζ increases with n_e for plasmas with nearly same T_e; see Fig. 7(a). The dependence of ζ on T_e was not clear since the variation of T_e was not enough. The dependence on n_e is also seen in the linearized Fokker-Planck calculation, but the experimental dependencies are stronger than those of calculations are.

The clear n_e dependence in the calculation should be explained under the linear theory. Fig. 8(a) shows damping of EC power as a function of major radius of ray trajectory. EC waves propagate from LFS (larger R) to HFS (smaller R) and are absorbed outside of cyclotron resonance due to Doppler shift. Flat T_e and n_e profiles are employed to ignore profile effects. CD location in the calculation is in HFS to ignore the trapped particle effect. The electron temperature is set to 5keV, and n_e is varied by 0.5, 1.0, and $2.0\times10^{19}/m^3$. The point where the EC power is damped by a half of total absorption power is considered to be a representative damping point. The point moves toward LFS, when n_e increases. This is because increased deposition of EC power to electrons with faster $v_{//}$ component, considering Doppler shift. Normalized ECCD efficiency is written by $\zeta \cdot Z_{\mathrm{eff}} = 3u^2$, when $u = (\omega - \omega_{\mathrm{ce}})/k_{//}v_{\mathrm{Te}}$ is much larger than unity under Lorentz approximation ($Z_{\mathrm{eff}} >> 1$) and without trapped particle effect [20]. Notations ω, ω_{ce}, $k_{//}$, v_{Te}, and Z_{eff} are angular frequency of wave, electron cyclotron angular frequency, wave number parallel to magnetic field, thermal velocity of electron, and effective charge, respectively. This analytical solution is compared to the calculation result (Fig. 8(b)), by using the ω_{ce} at point where the power is damped by a half of total absorption power. Results of linearized Fokker-Planck calculation agree well with the analytical solution. Therefore, the n_e dependence in calculation is considered to be due to the increase in wave coupling to faster $v_{//}$ electrons. When the absorption of EC waves moves faster $v_{//}$ in the velocity space, the absorption location apart from the trapping boundary by the toroidal effect. The ne dependence in Fig. 7(a) comes from both of the effects. The stronger

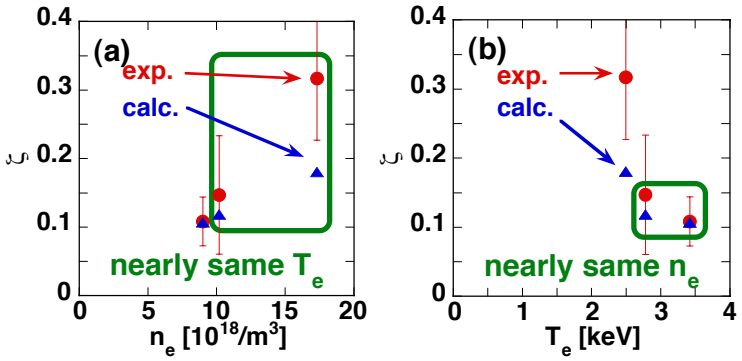

FIG. 7. Normalized CD efficiency by measurement (circle) and by calculation (triangle) as a function of (a) electron density, and of (b) electron temperature. Positive dependence of ζ on electron density is seen in (a), while dependence on T_e (b) is weaker than that on n_e.

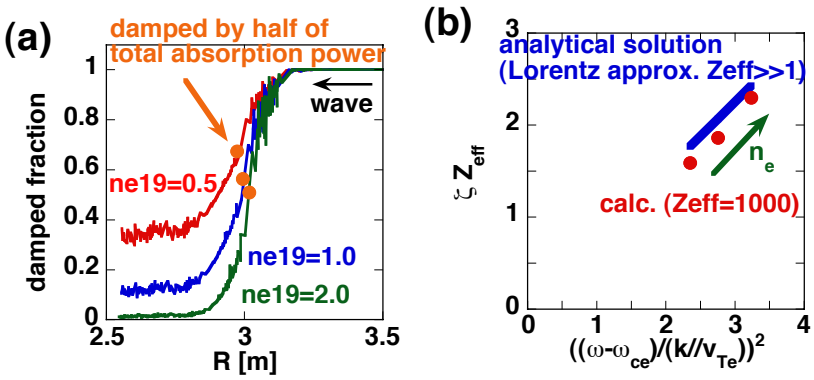

FIG. 8. Fraction of the EC power damped in the plasma, as a function of major radius. Location where EC waves damps by a half of total absorption power moves LFS of torus, when electron density increases. The shift is due to increased coupling of EC waves to electrons with larger $v_{//}$. Increase in ζ is consistent with the analytical solution under Lorentz approximation, which increases with $v_{//}$ of coupled electrons. In calculation, effective charge was set to 1000 for Lorentz approximation.

dependence of experiment than the linear theory is actually not known, so that we need further investigation of the reason. Both of the electric field effect and non-linear effect are not important in these experiments.

Further off-axis ECCD is also investigated, where the trapped particle effect is expected to be much stronger than ρ=0.35 in Fig. 6(b). Because the electron density is low (n_e~0.6x10^{19}m^{-3}) to enlarge the EC driven current density, we cannot compare the CD efficiency in the context of Fig. 6(b). We did not expect the previously described strong n_e dependence at the experiment. Measured EC driven current profiles are compared with calculations in Fig. 9. Figure 9(a) is for HFS deposition. Fig. 9(b) shows LFS deposition case, where the larger trapped particle effect is expected. Large errors in the experimental EC driven current show limitation of detecting a small non-inductive current by the loop voltage profile analysis in JT-60U. Measurement and calculation fairly agree well in CD location for LFS and HFS deposition. Again, EC driven current was smaller in LFS deposition than in HFS deposition, which can be the evidence of the trapped particle effect. Residual current density near the edge (ρ > 0.7) exists even in a phase without ECCD [2]. The residual current is considered to be due to errors in calibration of absolute angle of MSE diagnostics. Under the configuration of these discharges, normalized minor radius of 0.6 corresponds to trapped particle fraction of $\varepsilon^{0.5} = 0.4$, which is same to that of ρ=0.5 in ITER. ECCD in such a minor radius is important for applicable use on NTM suppression. Such further off-axis ECCD in LFS was

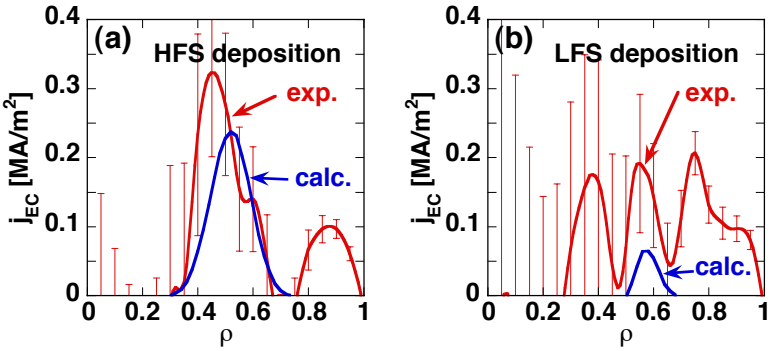

FIG. 9. EC driven current density profiles of measurement and of linearized Fokker-Planck calculation. (a) HFS deposition. (b) LFS deposition.

demonstrated.

5. Summary

Recent progress of EC system in JT-60U enabled production of a high electron temperature plasma, which is close to the ITER operation regime. The electron temperature at the plasma center reached 23keV with 2.9MW of EC waves. Spatially localized EC driven current profile was measured, which do not show significant radial diffusion of the driven current. Measurement of EC driven current at local T_e of 21keV showed that EC driven current is about 0.74MA, which is smaller than that of linearized Fokker-Planck calculation (1.1MA). The CD efficiencies in both experiment and calculation increase with T_e. Since the calculation does not include toroidal electric field effect and non-linearity, comparison of the measurement with calculation should be investigated in future considering both of them. Normalized CD efficiency ζ at ρ=0.35 of LFS deposition was about a half of that of HFS deposition, which is consistent with the calculation. The reduction of ζ can be an evidence of the trapped particle effect. Further off-axis ECCD in the same n_e to extend $\varepsilon^{0.5}$ will clarify the trapped particle effect. It was found that the normalized CD efficiency increases with the electron density. A part of the n_e dependence can be explained by a coupling of EC waves to a faster parallel velocity component of electrons. The stronger n_e dependence in experiment than in the calculation should be investigated. Further off-axis ECCD near $\varepsilon^{0.5}$ = 0.4 was demonstrated to show that the ECCD is effective even under such large trapped particle fraction.

References

[1] PETTY, C. C., et al., Nucl. Fusion **41** (2001) 551.
[2] SUZUKI, T., et al., Plasma Phys. Control. Fusion **44** (2002) 1.
[3] USHIGUSA, K., et al., Fusion Sci. Tech. **42** (2002) 255.
[4] ITER Final Design Report, Design Requirements and Guidelines (DRG) Level 1 (2001).
[5] ITER Physics Basis, Nuclear Fusion **39** (1999) 2498.
[6] ALIKAEV, V. V., et al., Nuclear Fusion **32** (1992) 1811.
[7] HARVEY, R. W., et al., Nuclear Fusion **37** (1997) 69.
[8] ISAYAMA, A., et al., Plasma Phys. Control. Fusion **42** (2000) L37.
[9] IKEDA, Y., et al., Nuclear Fusion **42** (2002) 375.
[10] IKEDA, Y., et al., Fusion Sci. Tech. **42** (2002) 435.
[11] SUGIE, T., et al., Fusion Sci. Tech. **42** (2002) 482.
[12] SEKI, M., et al., Fusion Sci. Tech. **42** (2002) 452.
[13] IDE, S., et al., Fusion Energy 1996, Proc. Int. Conf., Montreal (IAEA, Vienna, 1997) vol.3, 253.
[14] IDE, S., et al., Plasma Phys. Control. Fusion **44** (2002) A137.
[15] NAITO, O., et al., Phys. Rev. Lett. **89** (2002) 065001.
[16] FOREST, C. B., et al., Phys. Rev. Lett. **73** (1994) 2444.
[17] DNESTROVSKIJ, Yu. N., et al., Nuclear Fusion **28** (1988) 267.
[18] HARVEY, R. W., et al., Phys. Rev. Lett. **88** (2002) 205001.
[19] HARVEY, R. W., et al., Phys. Rev. Lett. **62** (1989) 426.
[20] CORDEY, J. G., et al., Plasma Physics **24** (1982) 73.